



Showcasing joint research from the Institute of Chemistry of Organometallic Compounds (ICCOM-CNR), Florence, Italy and l'Institut de chimie et procédés pour l'énergie, l'environnement et la santé (ICPEES-CNRS), Strasbourg, France.

Pyridine-decorated carbon nanotubes as a metal-free heterogeneous catalyst for mild CO₂ reduction to methanol with hydroboranes

The use of pyridine-decorated MWCNTs (N^{Py}-MW) as robust and reusable metal-free catalysts has been proposed as a benchmark heterogeneous system for CO₂ reduction with hydroboranes at ambient conditions (T = 294 K, P_{CO₂} = 1 atm) to afford MeOH upon hydrolysis of methyl borinate.

As featured in:



See C. Pham-Huu,
G. Giambastiani et al.,
Catal. Sci. Technol., 2017, 7, 5833.

Cite this: *Catal. Sci. Technol.*, 2017, 7, 5833Received 29th August 2017,
Accepted 27th October 2017

DOI: 10.1039/c7cy01772c

rsc.li/catalysis

Pyridine decorated multi-walled carbon nanotubes (N^{Py}-MW) have been successfully employed as a catalyst for the reduction of carbon dioxide to methyl borinate (R₂BO-CH₃) in the presence of 9-borabicyclo[3.3.1]nonane. N^{Py}-MW represents the first example of a heterogeneous, metal-free and durable catalyst for CO₂ hydroboration to methanol. A mechanistic cycle has been proposed on the basis of targeted blank experiments and a quantum chemical study, highlighting the non-innocent role played by the nanotube carrier in the final N^{Py}-MW catalytic performance.

The rapid growth of the world population and the steady increase of energy demand contrast with the limited nature of non-renewable resources, thus fostering a real worldwide energy crisis.¹ Moreover, mitigation of the effects caused by CO₂ overproduction represents one of the most urgent and challenging issues of modern society.² In this regard, in recent years, the scientists' point of view on carbon dioxide has radically changed. Nowadays, the chemical community does not regard CO₂ as a waste product from fossil fuels but rather as a chemical resource to be harvested and recycled into products of added value with the assistance of a catalyst.³ In particular, the catalytic conversion of CO₂ is highly attractive because it provides a synthetic fuel (CH₃OH) that can be exploited as an alternative energy source.⁴ Catalysts essentially based on transition metals have contributed to the establishment of seminal progress in the field of CO₂ fixation⁵ followed by its (photo-, electro-⁶ and/or chemical⁷) reduction

Pyridine-decorated carbon nanotubes as a metal-free heterogeneous catalyst for mild CO₂ reduction to methanol with hydroboranes†

G. Tuci,^a A. Rossin,^a L. Luconi,^a C. Pham-Huu,^{*b} S. Cicchi,^c
H. Ba^b and G. Giambastiani *^{ad}

to CO, formate or methanol. From a sustainable viewpoint, metal-free catalysts have emerged as highly attractive candidates to replace metal-based systems in the process. Given their reduced costs and limited environmental impact, metal-free catalysts have marked a real *paradigm shift* in “small molecule activation” research. Homogeneous frustrated Lewis pairs (FLPs),⁸ N-heterocyclic carbenes (NHC)⁹ and N-bases¹⁰ are known to interact with CO₂ and promote its catalytic deoxygenative hydroboration^{8a-d,f,9a,b,10,11} or hydrosilylation.^{9c,d} To date, heterogeneous metal-free systems for CO₂ reduction are almost exclusively limited to electrocatalysis, through the use of light-heterodoped (*i.e.* N, S) 1D and 2D carbon materials.¹² Although these authors are aware of the limits of this *chemical* approach to CO₂ reduction over other methods (in terms of energy efficiency, industrial practicality and impact of sacrificial reducing agents on the whole process), they feel that the development of robust, stable and efficient heterogeneous metal-free catalysts for CO₂ chemical conversion to methanol remains a highly attractive open challenge from a foundational viewpoint. In a recent finding, solid poly-N-heterocyclic carbene (poly-NHC) in combination with hydrosilanes has been shown to convert carbon dioxide to methanol selectively.¹³ However, the heterogeneous particles rapidly deactivate after a few cycles as a consequence of carbene protonation by gas impurities or silane.

In this study, we used pyridine-decorated MWCNTs (N^{Py}-MW) as a robust and reusable heterogeneous metal-free catalyst for CO₂ reduction with hydroboranes under ambient conditions ($T = 294$ K, $p_{\text{CO}_2} = 1$ atm) to afford methyl borinate. Its hydrolysis by means of an excess of water provides methanol (see the experimental section in the ESI† and Fig. S7). This class of exohedral N-functionalized nanotubes has recently been applied by us in the electrochemical oxygen reduction reaction (ORR).¹⁴ Besides their excellent performance in the ORR process, they served as unique models for the in-depth comprehension of the complex structure–reactivity relationships that drive the underlying O₂ reduction mechanism in these metal-free systems.^{14b,c} The recent outcomes in CO₂ hydroboration by homogeneous Lewis bases and the lack

^a Institute of Chemistry of Organometallic Compounds, ICCOM-CNR and Consorzio INSTM, Via Madonna del Piano, 10 – 50019, Sesto F.no, Florence, Italy. E-mail: giuliano.giambastiani@iccom.cnr.it

^b Institut de Chimie et Procédés pour l’Energie, l’Environnement et la Santé (ICPEES), UMR 7515 CNRS - University of Strasbourg, 67087 Strasbourg Cedex 02, France. E-mail: cuong.pham-huu@unistra.fr

^c Dipartimento di Chimica “Ugo Schiff”, Università di Firenze, 50019, Sesto Fiorentino, Italy

^d Kazan Federal University, 420008 Kazan, Russian Federation

† Electronic supplementary information (ESI) available: Catalyst characterization, experimental section and computational details. See DOI: 10.1039/c7cy01772c



of benchmark heterogeneous systems for the process prompted us to explore N^{Py} -MW as a solid catalyst for CO_2 activation and its hydroboration to methyl borinate ($\text{R}_2\text{BO}-\text{CH}_3$).

Scheme 1 outlines the general reaction process. Pyridine-decorated MWCNTs (N^{Py} -MW) are prepared following literature procedures^{14a,b} and are firstly employed as heterogeneous metal-free systems for CO_2 reduction under mild conditions in the presence of various hydroboranes [$\text{HBR}_2 = \text{HBcat}$ (catecholborane), HBpin (pinacolborane) and 9-BBN (9-borabicyclo[3.3.1]nonane)] as reducing agents. The pyridine content in N^{Py} -MW has been inferred as the average N wt% measured from different surface and bulk characterization procedures (see Table S1 in the ESI†).

The catalytic performance of N^{Py} -MW with each hydroborane is qualitatively investigated by *in situ* $^{13}\text{C}\{^1\text{H}\}$ and ^{13}C -NMR spectroscopy at fixed times, using isotopically enriched $^{13}\text{CO}_2$ ($p = 1$ atm) at ambient temperature ($T = 294$ K). All experiments have been run in thf-d_8 , since tetrahydrofuran is the optimal solvent to obtain a homogeneous catalyst dispersion upon short-time tube sonication (see the experimental section in the ESI†). Although NMR-tube reactions do not represent the ideal conditions required for an efficient heterogeneous process, they offer a clear perspective on the best reducing agent for the process. As shown in Table 1 (see also Fig. S2–S4†), 9-BBN largely outperforms all other selected hydroboranes under these conditions, providing the highest $^{13}\text{CO}_2$ conversion and percentage of methyl borinate 3 (Table 1, entry 3). No evidence for the transient generation of boryl formate (1) is given from each run under these conditions. The markedly lower conversions measured with HBpin and HBcat compared to 9-BBN (Table 1, entries 1 and 2 vs. 3) are in line with related hydroborations from the literature using metal-¹⁵ and metal-free^{9a,10a} homogeneous catalysts. According to this preliminary screening, 9-BBN is selected as the benchmark reducing agent for the optimization of N^{Py} -MW in the catalytic CO_2 reduction. To this aim, catalytic trials are then run in a 14 mL stainless-steel reactor equipped

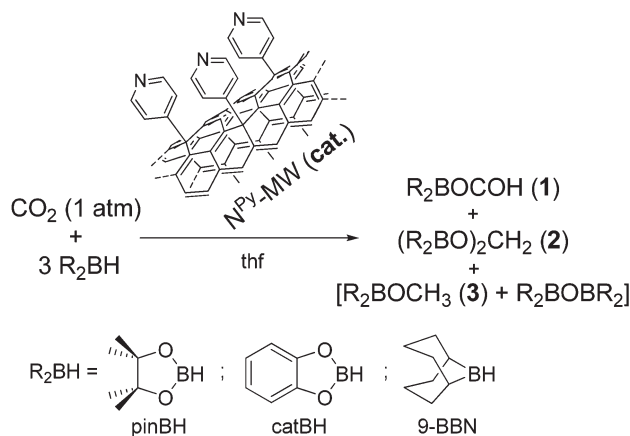
Table 1 Qualitative reduction study of CO_2 with various hydroboranes using N^{Py} -MW as catalyst^a

Entry	Borane	$^{13}\text{CO}_2^b$ (%)	1 ^b (%)	2 ^b (%)	3 ^b (%)
1	HBpin	96	—	4	n.d.
2	HBcat	~100	—	n.d.	n.d.
3	9-BBN	16	—	72	12

^a Reaction conditions: NMR tube equipped with a J. Young valve, charged with: 3 mg of catalyst (0.003 mmol; 0.75 mol%), 3.2 eq. of borane, 1 mL of thf-d_8 , 1 atm $^{13}\text{CO}_2$; 294 K, 24 h. ^b Based on the integration of the relative $^{13}\text{C}\{^1\text{H}\}$ signals (see the experimental section in the ESI).

with a glass sample holder, a magnetic stirrer bar and an external pressure control (3 atm at full scale).

Unless otherwise stated, all reactions were performed in thf-d_8 and their course was monitored at fixed times by analyzing the crude mixtures *via* $^{13}\text{C}\{^1\text{H}\}$ NMR spectroscopy in the presence of an internal standard (see the experimental section in the ESI†). Fig. 1 outlines the distribution of the reaction products over time and Table 2 summarizes the catalyst's performance as TON and TOF values. As shown in Fig. 1, CO_2 is steadily transformed into 1,1'-methylene diborinate 2 and methyl borinate 3 with complete conversion to the latter after 55 h (Table 2, entries 1–4). No traces of boryl formate 1 are detected at any reaction time. This confirms the kinetic control of the first reduction step and the rapid conversion of the transient intermediate 1 into the acetal 2 under ambient conditions.^{10a} After 36 h, CO_2 is entirely converted into 2 and 3 (Table 2, entry 2) and a 10/90 ratio in favor of methyl borinate 3 is measured after a reaction time of 43 h, corresponding to a TON value of 308 (for 3, based on the formed C–H bonds; Table 2, entry 3). To take full advantage of the catalyst performance, the same amount of N^{Py} -MW is suspended in 6 mL of thf and used for CO_2 reduction under ambient conditions ($T = 294$ K, $p_{\text{CO}_2} = 1$ atm) in a 60 mL volume reactor. Under these conditions, a TON value of



Scheme 1 CO_2 reduction catalyzed by N^{Py} -MW with various hydroboranes and the distribution of products (1–3). See also Fig. 1.

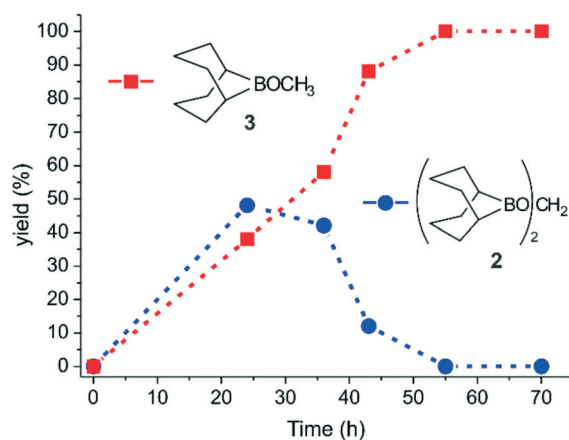


Fig. 1 Product distribution (%) over time (h) for the catalytic reduction of CO_2 (1 bar) with N^{Py} -MW as the catalyst and 9-BBN as the reducing agent. Yields (%) of 2 and 3 are from entries 1–4 of Table 2.



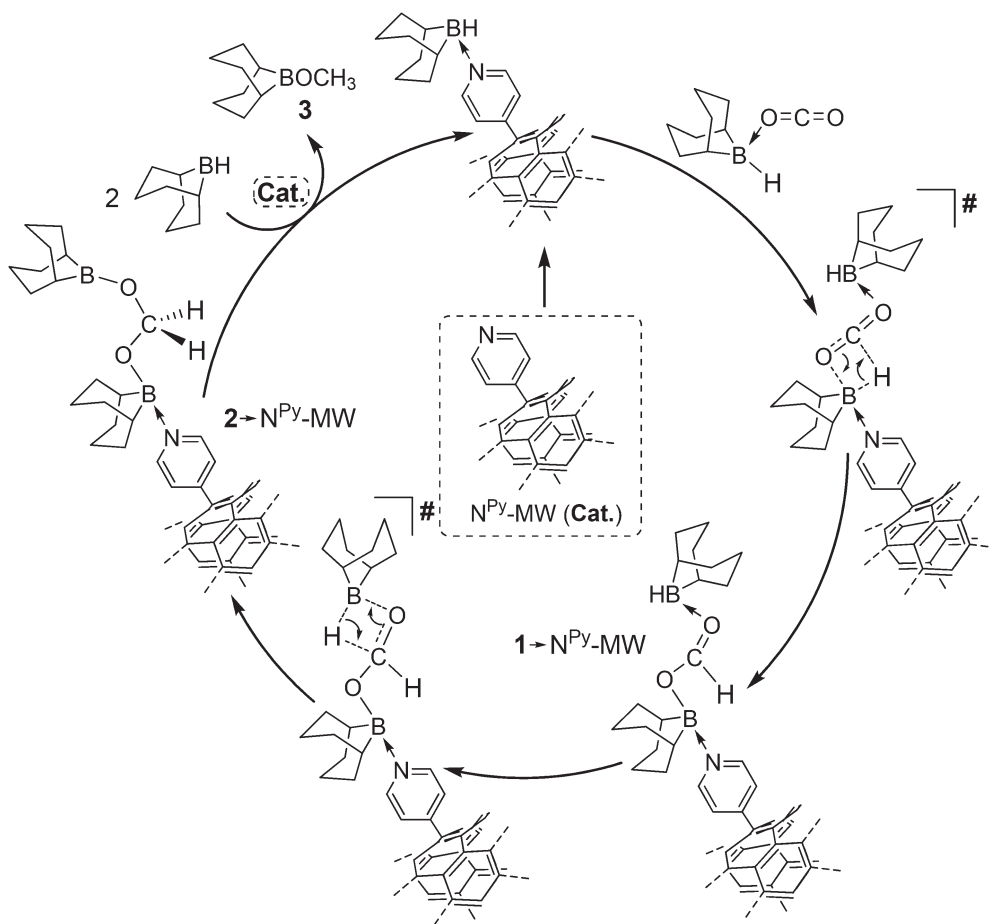
Table 2 Catalytic CO₂ reduction with N^{Py}-MW as the catalyst and 9-BBN as the reducing agent^a

Entry	Cat.	T (h)	2 ^b (%)	3 ^b (%)	MeOBBN (3)	
					TON ^c	TOF ^d
1	N ^{Py} -MW	24	48	38	130	5.4
2	N ^{Py} -MW	36	42	58	198	5.5
3	N ^{Py} -MW	43	10	90	308	7.2
4	N ^{Py} -MW	55	—	100	—	—
5 ^e	N ^{Py} -MW	96	16	84	1141	11.9
6	—	43	—	—	—	—
7 ^f	N ^{Py} -MW	43	13	87	298	6.9
8 ^g	N ^{Py} -MW	43	10	89	304	7.1
9 ^h	Pyridine	43	—	<1	n.d.	n.d.
10 ⁱ	MW	43	—	—	—	—

^a Reaction conditions (unless otherwise stated): 14 mL stainless-steel/Teflon®-lined reactor charged with 4.5 mg of catalyst (0.005 mmol; 0.3 mol%), 0.22 g of 9-BBN (3.2 eq.), 1.5 mL of thf-*d*₆, 1 atm CO₂; 294 K. ^b Based on the integration of ¹³C{¹H} signals using CH₃CN (30 μL, 0.57 mmol) as the internal standard (see the experimental section and Fig. S5 in the ESI). ^c Expressed as mmol_{MeOH} mmol_{cat}⁻¹ and calculated on the basis of the number of C-H bonds in 3. ^d Expressed as TON per h. ^e 60 mL reactor, 6 mL thf (2 mL thf-*d*₆ + 4 mL thf), 120 μL (2.28 mmol) CH₃CN as the internal standard. ^f 3rd recycling test. ^g 10th recycling test. ^h Pyridine as the catalyst (0.05 mmol; 3 mol%). ⁱ 5 mg of pristine MWCNTs as the catalyst.

1141 (based on C-H; Table 2, entry 5) is measured for 3 after 96 h (see experimental details in the ESI†).

Although a direct comparison with other metal or metal-free homogeneous catalysts is difficult because of the heterogeneous nature of N^{Py}-MW and the different experimental conditions used (temperature, pressure and reducing agent),¹⁶ it can be inferred that the TON values measured with N^{Py}-MW outperform (with very few exceptions¹⁷) those claimed for many single-site transition¹⁸ and main group¹⁹ metal complexes as homogeneous catalysts of the *state-of-the-art* (Table S2†). Recent findings in the field of metal-free catalysis have unveiled the excellent potentiality of selected Lewis bases in hydroboration (Table S2†). However, all the homogeneous systems pose several constraints and limitations to their exploitation as stable and reusable catalysts. N^{Py}-MW is easily recovered and reused in the hydroboration process and it maintains its catalytic performance, virtually unchanged even after ten successive runs (Table 2, entries 7 and 8 and Fig. S6 in the ESI†). No appreciable pyridine loss was measured on the recovered catalyst after several catalytic runs thus confirming the robustness of N^{Py}-MW for the hydroboration process (Fig. S1 and Table S1 in the ESI†). With TON values higher than those claimed for the majority

**Scheme 2** Proposed mechanism for the CO₂ reduction catalyzed by N^{Py}-MW in the presence of 9-BBN. See the ESI† for details on DFT calculations related to the postulated reaction path.

of homogeneous single-site transition and main group metal complexes of the *state-of-the-art*, N^{Py}-MW constitutes the first example of a durable, heterogeneous and metal-free catalyst for CO₂ hydroboration to methanol (Table S2†). Its catalytic performance also ranks among TON values with the same order of magnitude as those reported for selected and well known homogeneous, metal-free systems (Table S2†).

In a previous literature outcome, a pyridine derivative, [4-dimethylaminopyridine (DMAP)],^{10a} has shown only negligible catalytic performance as a homogeneous system in the hydroboration process. This result suggests that the role of the carbon nanotubes in N^{Py}-MW goes far beyond that of a simple and innocent carrier for the dangling pyridine active arms. In addition, we have proved that neither pristine MW carbon nanotubes (as a heterogeneous system) nor an excess of free pyridine (as a homogeneous catalyst) shows any appreciable catalytic performance under the optimized reaction conditions (Table 2, entries 9 and 10). While the first “blank” trial rules out any catalytic contribution from the C-nanomaterial as such (including that potentially rising from metal impurities present in trace amounts within its tridimensional network), the second experiment unambiguously demonstrates the existence of synergistic and beneficial effects between the C-nanocarrier and the covalently grafted N^{Py} groups. The identification of such effects starts from the comprehension of the underpinning reaction mechanism for the N^{Py}-MW mediated CO₂ hydroboration. The clear-cut identity of the surface N-groups along with the well-established functionalization protocol²⁰ used for their covalent grafting facilitates the elucidation of the presumed mechanistic path. The proposed catalytic cycle for the CO₂ hydroboration reaction is outlined in Scheme 2 and supported by model DFT calculations including thf solvent effects as a *continuum* (see the DFT study in the ESI†). The computational modeling carried out on the plain pyridine group‡ as the catalyst in the presence of CO₂ and two equivalents of 9-BBN (Scheme S1†) has confirmed the kinetically sluggish CO₂ conversion ($\Delta G^\ddagger = 26.7 \text{ kcal mol}^{-1}$ – RDS and Table 2 entry 9) into the thermodynamically favored adduct 1-NPy. The latter is supposed to undergo a rapid intramolecular hydroboration of the formyl unit to give 2-NPy through a kinetically and thermodynamically favored process. This result explains the rapid consumption of the formyl adduct whose presence has never been detected spectroscopically for any N^{Py}-MW mediated catalysis. The last step (third hydroboration) is thermodynamically downhill ($\Delta G = -35.4 \text{ kcal mol}^{-1}$) to give methyl borinate 3. The relatively high energy barrier measured for the first hydroboration step (rate determining step, RDS)^{10a,16} justifies the negligible activity of the homogeneous pyridine as the catalyst under ambient conditions (Table 2, entry 9). However, it contrasts with the catalytic performance of its heterogenized counterpart (N^{Py}-MW). The introduction of a negative charge in the simplified quantum chemical model based on plain pyridine as the

catalyst unveils an appreciable reduction of the energy barrier associated with the RDS of the process (Scheme S1† – red line). Accordingly, it can be inferred that the nanotubes act as electronic lungs for the surface grafted pyridine groups, boosting the nanotube-to-pyridine electronic density migration. Such an effect perfectly matches with experimental evidence outlined by Strano and co-workers on related covalently grafted aryl moieties at the nanotube sidewall.²¹ Therefore, a synergistic and positive interaction between the nanotube framework and the covalently grafted pyridine arms can be invoked as the rationale for the largely increased catalytic activity of the heterogenized heterocycles.

Conclusions

In summary, we have described the first example of a durable heterogeneous catalyst as a metal-free system for CO₂ hydroboration to methyl borinate 3 under ambient conditions. With turn-over numbers close to those claimed for other metal and metal-free homogeneous catalysts of the *state-of-the-art* and its effective re-use in catalysis, N^{Py}-MW candidates as a heterogeneous benchmark for this process. In addition, a hydroboration mechanism has been proposed on the joint basis of experimental data and *ab initio* simulations, suggesting the key role of the carbon nanotube carrier as an electronic reservoir for the dangling pyridine active arms. The latter point paves the way to the future exploitation of our catalyst technology, towards more sustainable leaf-like photo-electrocatalytic cells²² for CO₂ conversion into products of added value.

Conflicts of interest

There are no conflicts to declare.

Acknowledgements

The Italian MIUR through the PRIN 2015 Project SMARTNESS (2015K7FZLH) “Solar driven chemistry: new materials for photo- and electro-catalysis” is gratefully acknowledged for financial support. G. T. thanks Fondazione CR Firenze for its support to the HORIZON project. G. G. gratefully thanks Prof. G. Pacchioni and Dr. F. Mercuri for fruitful discussions.

Notes and references

‡ The authors have intentionally limited their DFT study to a single pyridine (bearing a zero and –1 charge) and its interaction with the reagents without including the CNT carrier. This choice stems from the need of postulating the electronic contribution of the macromolecular carrier without taking into account the unpredictable grafting mode (and related chemical surroundings) of the heterocycles to its outer surface. Any modelling of the N^{Py}-MW real system would necessarily imply an arbitrary choice of the pyridine chemical surroundings depending on its covalent anchoring (radical attack or radical displacement) to the CNT basal plane, edge sites or topological defects.



- 1 S. Chu, Y. Cui and N. Liu, *Nat. Mater.*, 2017, **16**, 16.
- 2 (a) D. R. Feldman, W. D. Collins, P. J. Gero, M. S. Torn, E. J. Mlawer and T. R. Shippert, *Nature*, 2015, **519**, 339; (b) M. E. Mann, *Proc. Natl. Acad. Sci. U. S. A.*, 2009, **106**, 4065.
- 3 G. A. Ozin, *Energy Environ. Sci.*, 2015, **8**, 1682.
- 4 (a) W. Wang, S. Wang, X. Ma and J. Gong, *Chem. Soc. Rev.*, 2011, **40**, 3703; (b) M. Aresta, *Carbon Dioxide as Chemical Feedstock*, Wiley-VCH Verlag GmbH & Co. KGaA, betz-druck GmbH, Darmstadt, 2010.
- 5 K. Huang, C.-L. Sun and Z.-J. Shi, *Chem. Soc. Rev.*, 2011, **40**, 2435.
- 6 (a) J. L. White, M. F. Baruch, J. E. Pander III, Y. Hu, I. C. Fortmeyer, J. E. Park, T. Zhang, K. Liao, J. Gu, Y. Yan, T. W. Shaw, E. Abelev and A. B. Bocarsly, *Chem. Rev.*, 2015, **115**, 12888; (b) D. D. Zhu, J. L. Liu and S. Z. Qiao, *Adv. Mater.*, 2016, **28**, 3423; (c) B. Khezri, A. C. Fisher and M. Pumera, *J. Mater. Chem. A*, 2017, **5**, 8230.
- 7 W.-H. Wang, Y. Himeda, J. T. Muckerman, G. F. Manbeck and E. Fujita, *Chem. Rev.*, 2015, **115**, 12936.
- 8 (a) F.-G. Fontaine, M.-A. Courtemanche and M.-A. Légaré, *Chem. – Eur. J.*, 2014, **20**, 2990; (b) G. Ménard and D. W. Stephan, *J. Am. Chem. Soc.*, 2010, **132**, 1796; (c) M.-A. Courtemanche, M.-A. Légaré, L. Maron and F.-G. Fontaine, *J. Am. Chem. Soc.*, 2013, **135**, 9326; (d) M.-A. Courtemanche, M.-A. Légaré, L. Maron and F.-G. Fontaine, *J. Am. Chem. Soc.*, 2014, **136**, 10708; (e) T. Wang and D. W. Stephan, *Chem. Commun.*, 2014, **50**, 7007; (f) A. Tlili, A. Voituriez, A. Marinetti, P. Thuéry and T. Cantat, *Chem. Commun.*, 2016, **52**, 7553; (g) R. Declercq, G. Bouhadir, D. Bourissou, M.-A. Légaré, M.-A. Courtemanche, K. S. Nahi, N. Bouchard, F.-G. Fontaine and L. Maron, *ACS Catal.*, 2015, **5**, 2513.
- 9 (a) S. C. Sau, R. Bhattacharjee, P. K. Vardhanapu, G. Vijaykumar, A. Datta and S. K. Mandal, *Angew. Chem., Int. Ed.*, 2016, **55**, 15147; (b) T. Wang and D. W. Stephan, *Chem. – Eur. J.*, 2014, **20**, 3036; (c) S. N. Riduan, Y. Zhang and J. Y. Ying, *Angew. Chem., Int. Ed.*, 2009, **48**, 3322; (d) F. Huang, G. Lu, L. Zhao, H. Li and Z.-X. Wang, *J. Am. Chem. Soc.*, 2010, **132**, 12388.
- 10 (a) C. Das Neves Gomes, E. Blondiaux, P. Thuéry and T. Cantat, *Chem. – Eur. J.*, 2014, **20**, 7098; (b) N. von Wolff, G. Lefèvre, J.-C. Berthet, P. Thuéry and T. Cantat, *ACS Catal.*, 2016, **6**, 4526.
- 11 T. Wanga and D. W. Stephan, *Chem. Commun.*, 2014, **50**, 7007.
- 12 (a) B. Kumar, M. Asadi, D. Pisasale, S. Sinha-Ray, B. A. Rosen, R. Haasch, J. Abiade, A. L. Yarin and A. Salehi-Khojin, *Nat. Commun.*, 2013, **4**, 3819; (b) J. Wu, R. M. Yadav, M. Liu, P. P. Sharma, C. S. Tiwary, L. Ma, X. Zou, X.-D. Zhou, B. I. Yakobson, J. Lou and P. M. Ajayan, *ACS Nano*, 2015, **9**, 5364; (c) X. Sun, X. Kang, Q. Zhu, J. Ma, G. Yang, Z. Liu and B. Han, *Chem. Sci.*, 2016, **7**, 2883.
- 13 S. N. Riduan, J. Y. Ying and Y. Zhang, *J. Catal.*, 2016, **343**, 46.
- 14 (a) G. Tuci, C. Zafferoni, P. D'Ambrosio, S. Caporali, M. Ceppatelli, A. Rossin, T. Tsoufis, M. Innocenti and G. Giambastiani, *ACS Catal.*, 2013, **3**, 2108; (b) G. Tuci, C. Zafferoni, A. Rossin, A. Milella, L. Luconi, M. Innocenti, L. Truong Phuoc, C. Duong-Viet, C. Pham-Huu and G. Giambastiani, *Chem. Mater.*, 2014, **26**, 3460; (c) G. Tuci, C. Zafferoni, A. Rossin, L. Luconi, A. Milella, M. Ceppatelli, M. Innocenti, Y. Liu, C. Pham-Huu and G. Giambastiani, *Catal. Sci. Technol.*, 2016, **6**, 6226; (d) G. Tuci, L. Luconi, A. Rossin, E. Berretti, H. Ba, M. Innocenti, D. Yakhvarov, S. Caporali, C. Pham-Huu and G. Giambastiani, *ACS Appl. Mater. Interfaces*, 2016, **8**, 30099.
- 15 S. Pereira and M. Srebnik, *Organometallics*, 1996, **14**, 3127.
- 16 S. Bontemps, *Coord. Chem. Rev.*, 2016, **308**, 117.
- 17 (a) S. Chakraborty, J. Zhang, J. A. Krause and H. Guan, *J. Am. Chem. Soc.*, 2010, **132**, 8872; (b) T. Liu, W. Meng, Q.-Q. Ma, J. Zhang, H. Li, S. Li, Q. Zhao and X. Chen, *Dalton Trans.*, 2017, **46**, 4504.
- 18 (a) S. Bontemps, L. Vendier and S. Sabo-Etienne, *J. Am. Chem. Soc.*, 2014, **136**, 4419; (b) S. Bontemps, L. Vendier and S. Sabo-Etienne, *Angew. Chem., Int. Ed.*, 2012, **51**, 1671; (c) M. J. Sgro and D. W. Stephan, *Angew. Chem., Int. Ed.*, 2012, **51**, 11343; (d) A. Aloisi, J.-C. Berthet, C. Genre, P. Thuéry and T. Cantat, *Dalton Trans.*, 2016, **45**, 14774.
- 19 (a) M. D. Anker, M. Arrowsmith, P. Bellham, M. S. Hill, G. Kociok-Kohn, D. J. Liptrot, M. F. Mahon and C. Weetman, *Chem. Sci.*, 2014, **5**, 2826; (b) J. A. B. Abdalla, I. M. Riddlestone, R. Tirfoin and S. Aldridge, *Angew. Chem., Int. Ed.*, 2015, **54**, 5098.
- 20 (a) J. L. Bahr and J. M. Tour, *Chem. Mater.*, 2001, **13**, 3823; (b) M. S. Strano, C. A. Dyke, M. L. Usrey, P. W. Barone, M. J. Allen, H. Shan, C. Kittrell, R. H. Hauge, J. M. Tour and R. E. Smalley, *Science*, 2003, **301**, 1519.
- 21 C. Fantini, M. L. Usrey and M. S. Strano, *J. Phys. Chem. C*, 2007, **111**, 17941.
- 22 S. Bensaid, G. Centi, E. Garrone, S. Perathoner and G. Saracco, *ChemSusChem*, 2012, **5**, 500.

